Hyperfine transitions in He-like ions as a tool for nuclear-spin-dependent parity-nonconservation studies

Fabrizio Ferro,[1,2,*] Andrey Surzhykov,[1,2] and Thomas Stöhlker[1,2,3]
[1]*Physikalisches Institut, Universität Heidelberg, Germany*
[2]*GSI Helmholtzzentrum für Schwerionenforschung, Darmstadt, Germany*
[3]*Helmholtz-Institut Jena, Jena, Germany*
(Received 21 March 2011; published 25 May 2011)

In this paper a scheme is proposed for measuring nuclear-spin-dependent parity-nonconservation effects in highly charged ions. The idea is to employ circularly polarized laser light for inducing the transition between the level $(1s2s)\,^1S_0$ and the hyperfine sublevels of $(1s2s)\,^3S_1$ in He-like ions with nonzero nuclear spin. We argue that an interference between the allowed magnetic dipole $M1$ and the parity-violating electric dipole $E1$ decay channel leads to an observable asymmetry of order 10^{-7} in the transition cross section, in the atomic range $28 \leqslant Z \leqslant 35$. Experimental requirements for asymmetry measurements are discussed in the case of He-like $^{77}_{34}$Se.

DOI: 10.1103/PhysRevA.83.052518 PACS number(s): 31.30.Gs, 31.15.am, 11.30.Er

I. INTRODUCTION

Atomic parity nonconservation (PNC) is known to be a versatile tool for testing the neutral-current hadronic part of the weak interaction at low energy. Special attention has been devoted to this interaction for its sensitiveness to new physics beyond the standard model of particles, which manifests itself in the violation of fundamental symmetries [1–3].

The PNC interaction is P odd, T even, and flavor conserving. The effective Hamiltonian of the PNC electron-nucleus interaction can be cast in the form [4]

$$H_{\rm PNC} = \frac{G_F}{\sqrt{2}}\left(-\frac{Q_W}{2}\gamma_5 + \frac{\kappa}{I}\boldsymbol{\alpha}\cdot\mathbf{I}\right)\rho(\mathbf{r}), \qquad (1)$$

where G_F is the Fermi constant, $\mathbf{I}$ the nuclear spin vector, and ρ the density of nucleons normalized to unity. Besides, the factors Q_W and κ characterize, respectively, contributions of the nuclear-spin-independent (nsi) and nuclear-spin-dependent (nsd) parts of the Hamiltonian (1). The nsd interaction, due to its explicit dependence on I, is only active in $I \neq 0$ nuclei, while the nsi one is always present. The tensor properties of the two parts of the Hamiltonian are defined by the pseudoscalar $\gamma_5 = i\gamma_0\gamma_1\gamma_2\gamma_3$ and the vector $\alpha_i = \gamma_0\gamma_i$ (with $i = 1,\ldots,3$), where $\gamma_0,\ldots,\gamma_3$ are the Dirac matrices.

The nuclear-spin-independent and nuclear-spin-dependent parts of the PNC Hamiltonian are of different physical origins. The nsi term arises from the exchange of Z_0 bosons between nucleons and atomic electrons. Since this is the dominant contribution in atomic PNC, it has attracted until now the most experimental and theoretical efforts (see, e.g., the review [5]). Instead, the nsd component principally comes from the magnetic interaction of an atomic electron with the nuclear anapole moment. The latter originates from parity-violating weak interactions among nucleons [6–8] that create spin and magnetic moment helixes in the nucleus [4]. Aside from the anapole moment, the nsd part in Eq. (1) also accounts for two other phenomena: one is generated by the combination of the usual nsi coherent Z_0 coupling together with the magnetic hyperfine interaction [9], and the other by the axial-coupling Z_0 exchange to the nucleus [9,10].

The joint effect of the nsd PNC contributions is very interesting because it offers access to the tiny and poorly understood spin and hyperfine dependences of PNC. The experimental analysis of such dependence is, however, a very complicated task, owing to the smallness of the nsd term in the effective Hamiltonian (1), if compared with the nsi one ($|Q_W| \sim 100|\kappa|$). Therefore, up to the present, only a single experiment has succeeded in unambiguously detecting nsd PNC in transitions between the hyperfine sublevels of $6s$ and $7s$ in ^{133}Cs with a 14% accuracy [11]. Furthermore, upper limits on the magnitude of the anapole moment of ^{205}Tl have also been ascertained [12], and future experiments in atomic traps have been recently proposed for Rb and Fr [13]. We stress that all these measurements make use of neutral heavy $I \neq 0$ atoms, where nsd PNC is enhanced by the $A^{2/3}$ scaling [8,9] with respect to the mass number A. Therefore, the assessment of the effective strength κ from the experimental findings requires, in general, detailed knowledge of the structure of neutral atoms. Due to the complicated multielectron structure in neutral heavy atoms, the total error on κ is dominated by that of theoretical calculations. We emphasize here that the need for accurate atomic structure calculations is not only a technical issue aiming at higher precision, rather it also has fundamental implications. In fact, the interpretation of measurements free of atomic-theory uncertainties is crucial to testing the electroweak theory in the low-energy regime [14].

To circumvent the atomic-structure complications of neutral atoms, one might explore nsd effects in highly charged ions. An evident advantage of this choice would be a significant improvement of the theoretical accuracy, ensured by the simple electron structure of highly charged ions. Moreover, it would be possible to employ high-precision spectroscopy techniques already available at ion storage rings [e.g., the experimental storage ring (ESR) at GSI]. Future experiments with highly charged ions will exploit the degeneracy of opposite-parity levels [15–19] to enhance PNC influence.

A possible scenario for studying nsd effects in highly charged ions has been proposed by Nefiodov *et al.* in Ref. [20]. In that work, a scheme employing a He-like ion beam in

*fabrizio.ferro@alice.de

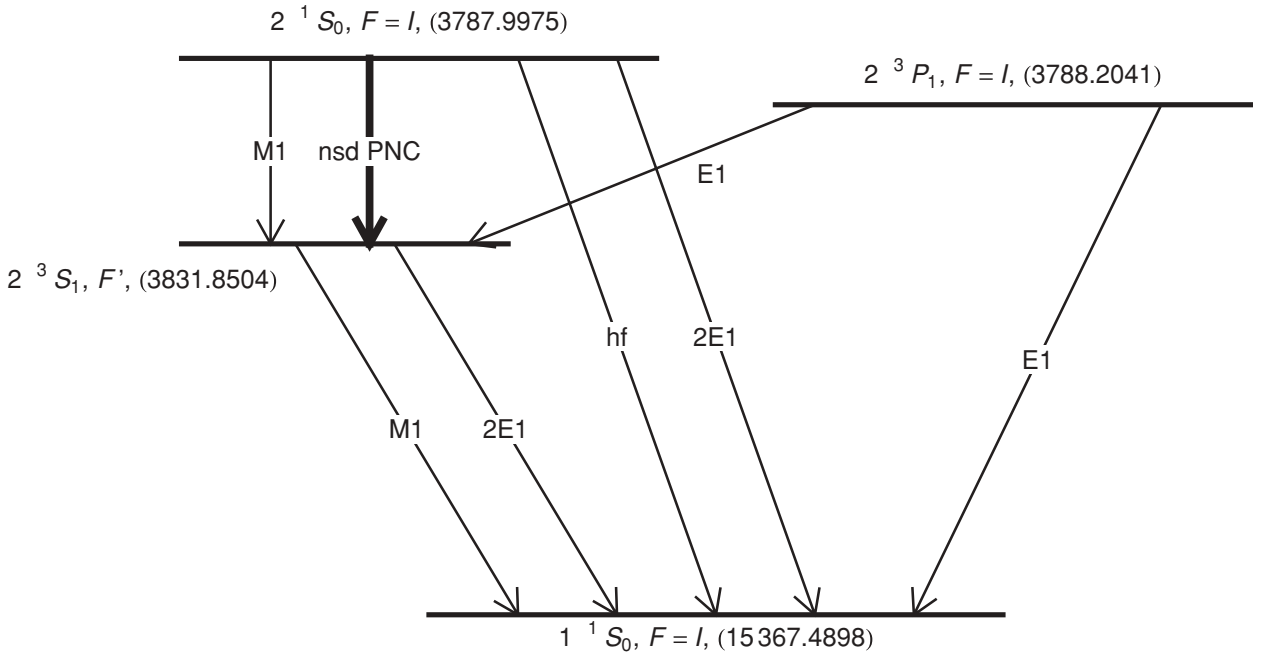

FIG. 1. Scheme of the first excited levels of He-like $^{77}_{34}$Se (not in scale). Energies in brackets are measured in eV, and F stands for the total angular momentum of any atomic state. Lines with arrows visualise the dominant electromagnetic transitions. The thick arrow line denoted "nsd PNC" represents the laser-induced transition considered in this paper.

the $(1s2s)\,^1S_0$ state was investigated. Owing to nsd PNC interaction, the states $(1s2s)\,^1S_0$ and $(1s2p)\,^3P_1$ mix in and, as a consequence, a small degree ($\sim 10^{-5}$) of polarization in the photons emitted from the $(1s2s)\,^1S_0 \to (1s^2)\,^1S_0$ spontaneous decay may appear. The difficulties in this observation scheme lie in the required polarization of the ion beam as well as in the detection of the evanescent polarization of the emitted photons. To overcome the latter critical points, we propose in this paper an alternative and promising scenario for measuring nsd phenomena. We shall focus in particular on He-like $^{77}_{34}$Se ions, where nsd PNC effects are markedly enhanced, for reasons that will be clarified in the next sections. A low-energy level scheme of this ion is sketched in Fig. 1. The idea is to prepare *unpolarized* ions in the $(1s2s)\,^1S_0$ state and *induce* an $E1$ transition to the $(1s2s)\,^3S_1$ state with circularly polarized laser light, in competition with the spontaneous $M1$ one. An easy tagging of this process would be the $M1$ decay of $(1s2s)\,^3S_1$ to the ground state, accompanied by emission of an 11.5 keV photon. By performing this experiment alternately with left and right circularly polarized laser light, we will show that an asymmetry proportional to the nsd PNC interaction strength κ may be observed in the transition cross section. An extreme ultraviolet (EUV) laser [$\Delta E \equiv E(2\,^3S_1) - E(2\,^1S_0) \simeq 43.8$ eV, see Fig. 1] with an intensity $\sim 10^{11}$ W/cm^2 will be required for such an observation. A similar scheme was recently proposed by Shabaev *et al.* [21] to investigate nuclear spin-independent PNC effects. Here, instead, we shall focus on the nsd PNC only.

This paper is organized as follows. In Secs. II and III, we discuss the parameters of the nsd PNC Hamiltonian and evaluate the mixing between the states $(1s2s)\,^1S_0$ and $(1s2p)\,^3P_1$. In Sec. IV we present the method employed to assess the hyperfine splitting of the first excited levels in He-like ions. The theoretical treatment of nsd PNC asymmetry in the cross section of the laser-induced transition $(1s2s)\,^1S_0 \to (1s2s)\,^3S_1$ is then developed in detail in Sec. V. A discussion of experimental requirements follows in Sec. VI, while conclusions are drawn in Sec. VII. Relativistic units ($\hbar = c = 1$) will be adopted throughout this paper.

II. NUCLEAR-SPIN-DEPENDENT PARITY NONCONSERVATION

In this work, we shall concentrate on the effects of PNC mixing between the opposite-parity states $2\,^1S_0 \equiv (1s2s)\,^1S_0$ and $2\,^3P_1 \equiv (1s2p)\,^3P_1$, in nuclei with spin $I \neq 0$ and atomic number $28 \leqslant Z \leqslant 36$. Since these two states have different total angular momenta, the mixing is mediated by the nsd part of the Hamiltonian (1) only, while any contribution from the nsi term is forbidden, as we will motivate in Sec. III. In principle, the nsi PNC interaction might be responsible for the mixing of $2\,^1S_0$ with $2\,^3P_0 \equiv (1s2p)\,^3P_0$, but this is strongly suppressed by a large energy separation of these states in the Z interval we are discussing [19]. Therefore, in the rest of this work, we shall focus on the nsd component only of the effective weak Hamiltonian (1), which we recall here for the sake of clarity [5,9,22]:

$$H_{\rm nsd}(\mathbf{r}) = \frac{G_F}{\sqrt{2}}\,\frac{\kappa}{I}\,\boldsymbol{\alpha}\cdot\mathbf{I}\,\rho(\mathbf{r}). \tag{2}$$

As already mentioned in the Introduction, three different effects contribute to the spin-dependent Hamiltonian in Eq. (2). Accordingly, the strength κ is usually parametrized in the form

$$\kappa = \frac{K}{I+1}\kappa_a - \frac{K-1/2}{I+1}\kappa_2 + \kappa_Q, \tag{3}$$

where the constant K reads

$$K = (-1)^{I+1/2-\ell}\left(I+\tfrac{1}{2}\right), \tag{4}$$

with ℓ being the total orbital angular momentum of the valence nucleons [5]. Although ℓ is in general poorly known, its value only discriminates the sign of K and, according to definition (3), the overall sign of the Hamiltonian $H_{\rm nsd}$ as well. However, as we will note in Sec. V, this is not a critical issue, and the actual sign of K could be extracted from experimental detection of the nsd PNC asymmetry. The strength κ is likewise weakly affected by the sign of K. Nevertheless, the relative variation of κ for $K = \pm(I+1/2)$ is always constrained below $\sim 3\%$.

In Eq. (3), the term κ_a describes the interaction of the nuclear anapole moment and is the dominant spin-dependent contribution [7]. The term κ_2 is the strength of the axial-coupling Z_0 exchange to the nucleus, while κ_Q denotes the effect of coherent Z_0 coupling to the nucleus perturbed by the hyperfine interaction [9,22]. As follows from Eq. (3), any further analysis of nsd PNC phenomena in He-like ions requires knowledge of the numerical value of the coefficients κ_a, κ_2, and κ_Q. For the ions in the interval $28 \leqslant Z \leqslant 36$, however, neither theoretical calculations nor experimental data about the aforementioned parameters are available. Therefore, in analogy with the treatment in Ref. [20], we will employ in this work the well-known $A^{2/3}$ scaling law [7,8]. We also note that the parameters κ_a, κ_2, and κ_Q reflect nuclear properties only, independent of the electronic structure of the system under investigation, and therefore they equally apply to both neutral atoms and ions. For neutral atoms, the best theoretical estimates of κ_a for the nuclide ^{133}Cs, including finite-size nuclear effects, is 0.362(62) [23,24], in agreement with the most accurate PNC experimental measurements [11,25]. For the same nuclide, the other two coefficients read $\kappa_2 = -0.063$ [26] and $\kappa_Q = 0.017$ [10]. We use the latter numerical values, rescaled to the A values of the ions considered in this work.

III. NUCLEAR-SPIN-DEPENDENT PNC MIXING OF $2\,^3P_1$ AND $2\,^1S_0$

Is it well known [17–19] that crossings of opposite-parity levels may be discovered in the low-energy spectrum of He-like ions for selected values of the atomic number Z. In particular, a quasidegeneracy of the two levels $2\,^3P_1$ and $2\,^1S_0$ occurs at $Z \sim 32$ [19]. This occurrence can be conveniently exploited in nsd PNC measurements. To demonstrate this, let us first recall a few relevant properties of the nsd PNC Hamiltonian $H_{\rm nsd}$ in Eq. (2). It contains two vectors, $\boldsymbol{\alpha}$ and $\mathbf{I}$, that operate in separate Hilbert spaces: $\boldsymbol{\alpha}$ in the space of the atomic wave functions, while $\mathbf{I}$ in that of the nuclear wave functions. Atomic states of opposite parity and total electron angular momenta J_1 and J_2 such that $J_1 - J_2 = \pm 1,0$, may be connected by operator $\boldsymbol{\alpha}$. Therefore, $2\,^3P_1$ and $2\,^1S_0$ can mix together through the effective nsd interaction. The latter property is rather peculiar if compared with the pseudoscalar nuclear-spin-independent Hamiltonian, which mixes states of opposite parity and *identical* total angular momentum ($J_1 - J_2 = 0$) only.

Owing to the Hamiltonian $H_{\rm nsd}$, the $2\,^1S_0$ atomic state in He-like ions with nuclear spin $I \neq 0$ can be described as

$$|2\,^1S_0, I, IM\rangle + i\eta|2\,^3P_1, I, F_1M_1\rangle, \tag{5}$$

where M is the magnetic quantum number of the coupled $2\,^1S_0$ state, while F_1 and M_1 stand, respectively, for the total angular momentum and magnetic number of the coupled state $2\,^3P_1$. The mixing coefficient $i\eta$ in Eq. (5) is expressed at leading order of perturbation theory by

$$\begin{aligned} i\eta &= \frac{\langle 2\,^3P_1, I, F_1M_1|H_{\rm nsd}(1)+H_{\rm nsd}(2)|2\,^1S_0, I, IM\rangle}{E(2\,^1S_0) - E(2\,^3P_1) - i[\Gamma(2\,^1S_0) - \Gamma(2\,^3P_1)]/2} \\ &= \frac{\langle 2\,^3P_1, I, F_1M_1|H_{\rm nsd}(1)+H_{\rm nsd}(2)|2\,^1S_0, I, IM\rangle}{E(2\,^1S_0) - E(2\,^3P_1)}, \end{aligned} \tag{6}$$

where E and Γ represent the level energy and width of each state. The notation $H_{\rm nsd}(i)$, with $i = 1,2$, means that the one-particle Hamiltonian operates on the i-th electron of He-like atomic states. The suppression of Γ terms in Eq. (6) is a consequence of time invariance [27], which demands that η be a real number.

By making use of standard angular momentum techniques, the matrix element in Eq. (6) simplifies as

$$\begin{aligned} &\langle 2\,^3P_1, I, F_1M_1|[\boldsymbol{\alpha}(1)+\boldsymbol{\alpha}(2)]\cdot\mathbf{I}\,\rho(\mathbf{r})|2\,^1S_0, I, IM\rangle \\ &= (-1)^{2I}\delta_{IF_1}\delta_{MM_1}\begin{Bmatrix} I & I & 1 \\ 1 & 0 & I \end{Bmatrix} \\ &\quad\times\langle 2\,^3P_1||[\hat{\alpha}(1)+\hat{\alpha}(2)]\rho(\mathbf{r})||2\,^1S_0\rangle\langle I||\hat{I}||I\rangle \\ &= -\delta_{IF_1}\delta_{MM_1}\sqrt{\frac{I(I+1)}{3}}\langle 2\,^3P_1||[\hat{\alpha}(1)+\hat{\alpha}(2)]\rho(\mathbf{r})||2\,^1S_0\rangle, \end{aligned} \tag{7}$$

since atomic and nuclear parts of the wave functions can be decoupled. The result in Eq. (7) imposes that the two coupled states $|2\,^3P_1, I, F_1M_1\rangle$ and $|2\,^1S_0, I, IM\rangle$ must have the same total angular momentum and magnetic number, i.e., $F_1 = I$ and $M_1 = M$. Above, as well as in the rest of the paper, we introduced the common notation $\langle a||\hat{V}||b\rangle$ to denote the reduced matrix element of a generic vector operator $\mathbf{V}$ between two states a,b. We also made use of $\langle I||\hat{I}||I\rangle = \sqrt{I(I+1)(2I+1)}$.

Although the atomic reduced matrix element $\langle 2\,^3P_1||[\hat{\alpha}(1)+\hat{\alpha}(2)]\rho(\mathbf{r})||2\,^1S_0\rangle$ is calculated between two-electron wave functions, it is also possible to express it in terms of one-particle matrix elements. While the state $2\,^1S_0$ can be treated in a single determinantal approach, i.e., $|2\,^1S_0\rangle = |(1s2s)_0\rangle$, the $2\,^3P_1$ requires us to include mixing between the configurations $(1s2p_{1/2})_1$ and $(1s2p_{3/2})_1$. Therefore, we pose

$$|2\,^3P_1\rangle = c_{2p_{1/2}}|(1s2p_{1/2})_1\rangle + c_{2p_{3/2}}|(1s2p_{3/2})_1\rangle, \tag{8}$$

where we calculated the coefficients $c_{2p_{1/2}}$ and $c_{2p_{3/2}}$ in the framework of relativistic many-body perturbation theory, as described in Ref. [18]. By employing Eq. (8), the reduced matrix element of the operator $[\hat{\alpha}(1)+\hat{\alpha}(2)]\rho(\mathbf{r})$ can be rewritten explicitly in terms of one-electron matrix elements

(see e.g., Ref. [28]) as

$$\begin{aligned}\langle 2^3P_1||[\hat{\alpha}(1)+\hat{\alpha}(2)]\rho||2^1S_0\rangle &= c_{2p_{1/2}}\langle (1s2p_{1/2})_1||[\hat{\alpha}(1)+\hat{\alpha}(2)]\rho||(1s2s)_0\rangle \\ &\quad + c_{2p_{3/2}}\langle (1s2p_{3/2})_1||[\hat{\alpha}(1)+\hat{\alpha}(2)]\rho||(1s2s)_0\rangle \\ &= c_{2p_{1/2}}\langle 2p_{1/2}||\hat{\alpha}\rho||2s\rangle + c_{2p_{3/2}}\langle 2p_{3/2}||\hat{\alpha}\rho||2s\rangle, \end{aligned} \tag{9}$$

where, with the help of the Wigner-Eckart theorem, explicit expressions of $\langle 2p_{1/2}||\hat{\alpha}\rho||2s\rangle$ and $\langle 2p_{3/2}||\hat{\alpha}\rho||2s\rangle$ are readily evaluated:

$$\begin{aligned}\langle 2p_{1/2}||\hat{\alpha}\rho||2s\rangle &= \sqrt{6}\,\langle 2p_{1/2},m=1/2|\alpha_z\rho|2s,m=1/2\rangle \\ &= -i\sqrt{6}\int_0^{+\infty} dr\, r^2\rho(r)\Big[f_{2p_{1/2}}(r)g_{2s}(r) \\ &\quad + \frac{1}{3}f_{2s}(r)g_{2p_{1/2}}(r)\Big], \end{aligned} \tag{10}$$

$$\begin{aligned}\langle 2p_{3/2}||\hat{\alpha}\rho||2s\rangle &= \sqrt{6}\,\langle 2p_{3/2},m=1/2|\alpha_z\rho|2s,m=1/2\rangle \\ &= -\frac{4i}{\sqrt{3}}\int_0^{+\infty} dr\, r^2\rho(r)f_{2s}(r)g_{2p_{3/2}}(r). \end{aligned} \tag{11}$$

In the explicit numerical calculations of Eqs. (10) and (11), the nuclear density ρ is chosen to be spherically symmetric and homogeneous. The large (g) and small (f) components of the Dirac wave functions $\psi_{n\kappa m}(\mathbf{r})$ come from the usual definition

$$\psi_{n\kappa m}(\mathbf{r}) = \begin{pmatrix} g_{n\kappa}(r)\Omega_{\kappa m}(\hat{\mathbf{r}}) \\ i f_{n\kappa}(r)\Omega_{-\kappa m}(\hat{\mathbf{r}}) \end{pmatrix}, \tag{12}$$

where $\kappa = (-1)^{j+l+1/2}(j+1/2)$.

From Eqs. (7), (9), (10), and (11), together with definitions (2) and (6), the PNC mixing coefficient $i\eta$ follows explicitly

$$\begin{aligned} i\eta = iG_F\frac{\kappa}{E(2^1S_0)-E(2^3P_1)}\sqrt{\frac{I+1}{I}}\Bigg[c_{2p_{1/2}} &\times\int_0^{+\infty} dr\, r^2\rho(r)\left(f_{2p_{1/2}}(r)g_{2s}(r)+\frac{1}{3}f_{2s}(r)g_{2p_{1/2}}(r)\right) \\ &+\frac{2\sqrt{2}}{3}c_{2p_{3/2}}\int_0^{+\infty} dr\, r^2\rho(r)f_{2s}(r)g_{2p_{3/2}}(r)\Bigg]. \end{aligned} \tag{13}$$

Table I reports a comparison of our numerical results of the mixing coefficient η with those in Ref. [20], for several nuclides with $29 \leqslant Z \leqslant 36$. After correcting for the hyperfine energy splitting $E(2^3P_1) - E(2^1S_0)$ with $F = I$ (which we calculated as discussed in Sec IV), a fair agreement is achieved. It is already evident from Table I that $^{77}_{34}$Se is a likely candidate for nsd PNC investigations, since it offers the largest mixing factor among the listed nuclides. We will, however, come back to the ion choice in Sec. VI.

IV. HYPERFINE LEVEL SPLITTING

We showed in the previous section that nsd PNC effects are inversely proportional to $\Delta E = E(2^1S_0) - E(2^3P_1)$ in He-like ions. Therefore, it is essential to accurately calculate the energy splitting between the $F = I$ hyperfine component of atomic levels 2^3P_1 and 2^1S_0. To this purpose, we consider the Hamiltonian

$$H = H_0 + H_{\rm hf}, \tag{14}$$

where H_0 describes the He-like ion without including any magnetic effect, and $H_{\rm hf}$ is the hyperfine perturbation in dipole approximation,

$$H_{\rm hf} = \mathbf{T}\cdot\mathbf{M}. \tag{15}$$

The vectors $\mathbf{T}$ and $\mathbf{M}$ act separately in the space of the electrons and of the nucleus. The electron operator $\mathbf{T}$ is defined in terms of the Dirac matrices and vector spherical harmonics (see e.g.,

TABLE I. Comparison of the numerical results for the weak mixing coefficient η, normalized to $\kappa_W \equiv \sqrt{2}\,\kappa\,(I+1)/K$, with those of Ref. [20] for several He-like ions in the region $29 \leqslant Z \leqslant 36$. Our $|\eta/\kappa_W|$ value is corrected by the factor $C_E = \Delta E/\Delta E_{\rm ref}$, where $\Delta E = E(2^3P_1) - E(2^1S_0)$ is our calculated energy splitting (see Sec. IV) and $\Delta E_{\rm ref}$ is that reported in Ref. [20]. For each ion, we list its nuclear spin and parity I^π.

Ion	I^π	$E(2^3P_1) - E(2^1S_0)$ (meV)	C_E	$10^{-10}1/C_E\lvert\eta/\kappa_W\rvert$ (this work)	$10^{-10}\lvert\eta/\kappa_W\rvert$ Ref. [20]
$^{63}_{29}$Cu	$3/2^-$	218.75	1.12914	2.13483	2.08
$^{65}_{29}$Cu	$3/2^-$	217.31	1.13663	2.13374	2.08
$^{67}_{30}$Zn	$5/2^-$	191.55	1.08066	2.93813	2.87
$^{69}_{31}$Ga	$3/2^-$	150.22	1.22487	3.93801	3.83
$^{71}_{31}$Ga	$3/2^-$	143.92	1.27849	3.93592	3.83
$^{73}_{32}$Ge	$9/2^+$	172.74	1.05361	4.51164	4.38
$^{75}_{33}$As	$3/2^-$	168.43	1.19930	4.84842	4.70
$^{77}_{34}$Se	$1/2^-$	206.58	1.19566	5.12805	4.97
$^{79}_{35}$Br	$3/2^-$	263.46	1.20322	4.12056	3.98
$^{81}_{35}$Br	$3/2^-$	260.51	1.21684	4.11812	3.98
$^{83}_{36}$Kr	$9/2^+$	399.99	1.03776	3.51849	3.41

Ref. [29]). Instead, **M** is connected to the nuclear magnetic moment μ, since it obeys the relation

$$\langle I||\hat{M}||I\rangle = \sqrt{\frac{(2I+1)(I+1)}{I}}\mu. \tag{16}$$

The matrix element of the Hamiltonian (14) between two states of atomic angular momentum J and J', and total angular momentum F reads

$$W^F_{J,J'} = E_J\delta_{JJ'} + (-1)^{I+J+F}\begin{Bmatrix} I & J & F \\ J' & I & 1 \end{Bmatrix}\langle J||\hat{T}||J'\rangle\langle I||\hat{M}||I\rangle, \tag{17}$$

where E_J is the unperturbed energy of the atomic state of angular momentum J.

Diagonalization of matrix $W^F_{J,J'}$ for any allowed F gives access to the energies of the hyperfine sublevels into which any state splits. To calculate the energies of the $2\,^3P_1$ multiplet, we considered mixing between the closely lying $2\,^3P_{0,1,2}$ and $2\,^1P_1$ levels. Numerical results are reported in Ref. [30] and, for the case of He-like $^{77}_{34}$Se, also in Fig. 1.

In contrast to the $2\,^3P_1$ multiplet, hyperfine corrections on the $2\,^1S_0$ state take place through mixing with $2\,^3S_1 \equiv (1s2s)\,^3S_1$ only. In the Z interval considered in this paper, however, the energy separation between even-parity states is large ($\simeq 56$ eV in $^{77}_{34}$Se, see Fig. 1) in comparison with that of the odd-parity states ($\simeq 2.7$ eV between $2\,^3P_0$ and $2\,^3P_1$ in $^{77}_{34}$Se [31]), and the hyperfine correction has been found correspondingly negligible. Therefore, we assume in the following that no shift affects the $2\,^1S_0$ energy, and that the three $F = I, I \pm 1$ hyperfine sublevels of $2\,^3S_1$ are degenerate. We will see in Sec. VI that this approximation is also motivated by experimental requirements.

The numerical values of the splitting $\Delta E = E(2\,^1S_0) - E(2\,^3P_1)$, complete with hyperfine corrections, are listed in Table I, for He-like ions in the range $29 \leqslant Z \leqslant 36$.

V. LASER-INDUCED $2\,^1S_0 \to 2\,^3S_1$ TRANSITION

In the previous sections we pointed out that the two levels $2\,^1S_0$ and $2\,^3P_1$ of He-like ions are quasidegenerate and their wave functions are mixed by a factor η due to the nsd PNC interaction. We will focus here on the consequences of this mixing upon the $2\,^1S_0 \to 2\,^3S_1$ transition induced by circularly polarized laser light. From the discussion, it will be clarified that forbidden transitions may take place and be experimentally observed. In particular, we will prove that the interference between the allowed $M1$ transition multipole (see Fig. 1) and the forbidden $E1$ gives rise to measurable effects, which are proportional to the nsd PNC strength.

To analyze the properties of the forbidden one-photon $2\,^1S_0 \to 2\,^3S_1$ transition, let us start by writing the cross section in the general form

$$\sigma = 4(2\pi)^3\frac{1}{2I+1}\sum_{M,M'}\frac{|\langle 2\,^3S_1, I, F'M'|R(1)+R(2)(|2\,^1S_0, I, IM\rangle + i\eta|2\,^3P_1, I, IM\rangle)|^2}{\Gamma_{2\,^3S_1}+\Gamma_{2\,^1S_0}}. \tag{18}$$

In this formula, we recalled that the initial state $2\,^1S_0$ is mixed with $2\,^3P_1$ as in Eq. (5), and we defined with Γ and M, respectively, the decay width and the magnetic number of the two levels. The hyperfine sublevel of the final state must satisfy the selection rule $|I-1| \leqslant F' \leqslant I+1$. The scalar one-particle operator R expresses the single-photon interaction $-e\boldsymbol{\alpha}\cdot\mathbf{A}$, where $\mathbf{A}$ is the vector potential

$$\mathbf{A}(\mathbf{x}) = \frac{\boldsymbol{\epsilon}\, e^{i\mathbf{k}\cdot\mathbf{x}}}{\sqrt{2\omega(2\pi)^3}}. \tag{19}$$

Here, the physical properties of the absorbed photon are expressed by the polarization direction $\boldsymbol{\epsilon}$, the angular velocity ω, and the wave vector $\mathbf{k}$. They obey the relations $|\mathbf{k}| = \omega$ and $\mathbf{k}\cdot\boldsymbol{\epsilon} = 0$. To describe circularly polarized laser light, we set [32]

$$\boldsymbol{\epsilon} = \frac{1}{\sqrt{2}}(\boldsymbol{\epsilon}_1 + i\lambda\boldsymbol{\epsilon}_2), \tag{20}$$

where the linear polarization vectors $\boldsymbol{\epsilon}_{1,2}$ are chosen in such a way that $\boldsymbol{\epsilon}_{1,2}\cdot\mathbf{k} = 0$ and $\boldsymbol{\epsilon}_1\cdot\boldsymbol{\epsilon}_2 = 0$. The helicity $\lambda = \pm 1$ in Eq. (20) is defined in such a way that the positive (negative) sign corresponds to right (left) circular polarization of the laser light.

As ensured by the smallness of the transition energy considered here, operator R reduces in first order to

$$R = -e\boldsymbol{\alpha}\cdot\mathbf{A} \approx -e\frac{\boldsymbol{\alpha}\cdot\boldsymbol{\epsilon}}{\sqrt{2\omega(2\pi)^3}}(1 + i\mathbf{k}\cdot\mathbf{x}). \tag{21}$$

From approximation (21), in the electromagnetic multipole expansion of operator R, only the electric dipole ($E1$), magnetic dipole ($M1$), and electric quadrupole ($E2$) terms are retained, while all higher orders disappear. Moreover, no electric-quadrupole contribution is allowed between the two levels under study, owing to angular momentum and parity conservation of the electromagnetic interaction. By taking this into account, the transition operator (21) simply reads

$$R = R_{E1} + R_{M1}. \tag{22}$$

Here, the $E1$ operator is defined as

$$R_{E1} = -i\omega\frac{\boldsymbol{\epsilon}\cdot\mathbf{d}}{\sqrt{2\omega(2\pi)^3}}, \tag{23}$$

with $\mathbf{d} = e\mathbf{r}$ being the electric dipole. The $M1$ operator instead reads

$$R_{M1} = i\frac{\boldsymbol{\epsilon}\times\mathbf{k}\cdot\boldsymbol{\mu}}{\sqrt{2\omega(2\pi)^3}}, \tag{24}$$

where $\boldsymbol{\mu} = e\,\mathbf{x} \times \boldsymbol{\alpha}/2$ is the magnetic dipole. As known in atomic structure calculations, the operator R_{E1} depends on the particular choice of the gauge for the coupling of the radiation field. In Eq. (23) we adopted the length gauge because, in this case, the zeroth-order approximation already accounts for the one-loop QED corrections in velocity gauge calculations, as was shown in Ref. [21].

From Eqs. (18) and (22), we get for the $2\,^1S_0 \to 2\,^3S_1$ cross section

$$\begin{aligned}\sigma(\eta) \propto \sum_{M,M'} &|\langle 2\,^3S_1, I, F'M'|R_{E1}(1) + R_{E1}(2) + R_{M1}(1) \\ &+ R_{M1}(2)(|2\,^1S_0, I, IM\rangle + i\eta|2\,^3P_1, I, IM\rangle)|^2 \\ &= |A|^2 + 2\eta\mathrm{Re}(AB^*) + O(\eta^2), \end{aligned} \tag{25}$$

where the tiny term proportional to η^2 is neglected. In Eq. (25), moreover, we introduced the short-hand notations

$$|A|^2 = \frac{\omega^2}{3}|\langle 2\,^3S_1, I, F'||\hat{\mu}(1) + \hat{\mu}(2)||2\,^1S_0, I, I\rangle|^2, \tag{26}$$

and

$$\begin{aligned}\mathrm{Re}(AB^*) = \frac{\omega\lambda}{3}&\langle 2\,^3S_1, I, F'||\hat{\mu}(1) + \hat{\mu}(2)||2\,^1S_0, I, I\rangle \\ &\times \langle 2\,^3P_1, I, I||\hat{d}(1) + \hat{d}(2)||2\,^3S_1, I, F'\rangle. \end{aligned} \tag{27}$$

The two terms $|A|^2$ and $\mathrm{Re}(AB^*)$ represent, respectively, the allowed $M1$ transition, and the interference between $M1$ and the parity-violating $E1$.

By decoupling atomic and nuclear parts in Eqs. (26) and (27), we obtain the explicit forms

$$\begin{aligned}|A|^2 &= \frac{\omega^2}{3}(2I+1)(2F'+1)\begin{Bmatrix} 1 & F' & I \\ I & 0 & 1 \end{Bmatrix}^2 \\ &\quad\times |\langle 2\,^3S_1||\hat{\mu}(1) + \hat{\mu}(2)||2\,^1S_0\rangle|^2 \\ &= \frac{\omega^2}{9}(2F'+1)|\langle 2\,^3S_1||\hat{\mu}(1) + \hat{\mu}(2)||2\,^1S_0\rangle|^2, \end{aligned} \tag{28}$$

and

$$\begin{aligned}&2\mathrm{Re}(AB^*) \\ &= (-1)^{3I+F'}\frac{\omega\lambda}{3}(2I+1)(2F'+1)\begin{Bmatrix} 1 & F' & I \\ I & 0 & 1 \end{Bmatrix}\begin{Bmatrix} 1 & I & I \\ F' & 1 & 1 \end{Bmatrix} \\ &\quad\times\langle 2\,^3S_1||\hat{\mu}(1) + \hat{\mu}(2)||2\,^1S_0\rangle\langle 2\,^3P_1||\hat{d}(1) + \hat{d}(2)||2\,^3S_1\rangle \\ &= (-1)^{2F'+1}\frac{\omega\lambda}{3}\sqrt{\frac{2I+1}{3}}(2F'+1)\begin{Bmatrix} 1 & I & I \\ F' & 1 & 1 \end{Bmatrix} \\ &\quad\times\langle 2\,^3S_1||\hat{\mu}(1) + \hat{\mu}(2)||2\,^1S_0\rangle\langle 2\,^3P_1||\hat{d}(1) + \hat{d}(2)||2\,^3S_1\rangle. \end{aligned} \tag{29}$$

By inserting expressions (28) and (29) into Eq. (25), we may cast the transition cross section to the final hyperfine sublevel of momentum F' in the presence of nsd PNC mixing $\eta \neq 0$ as

$$\sigma_{F'}(\eta) = (2F'+1)\sigma(0)(1 + \lambda\mathcal{K}_{F'}), \tag{30}$$

where the parity-preserving cross section reads

$$\sigma(0) = \frac{4(2\pi)^3\omega^2}{9(2I+1)}\frac{|\langle 2\,^3S_1||\hat{\mu}(1) + \hat{\mu}(2)||2\,^1S_0\rangle|^2}{\Gamma_a + \Gamma_b}, \tag{31}$$

and the parameter $\mathcal{K}_{F'}$ takes the form

$$\begin{aligned}\mathcal{K}_{F'} = \frac{2\omega\mathrm{Re}(AB^*)}{\lambda|A|^2} &= (-1)^{2F'+1}2\eta\sqrt{\frac{2I+1}{3}}\begin{Bmatrix} 1 & I & I \\ F' & 1 & 1 \end{Bmatrix} \\ &\quad\times\frac{c_{2p_{1/2}}\langle 2p_{1/2}||\hat{d}||2s\rangle + c_{2p_{3/2}}\langle 2p_{3/2}||\hat{d}||2s\rangle}{\langle 2s||\hat{\mu}||2s\rangle - \langle 1s||\hat{\mu}||1s\rangle}. \end{aligned} \tag{32}$$

We stress here that $\mathcal{K}_{F'}$ depends explicitly on the mixing coefficient η and, as a consequence of Eq. (13), on the effective nsd PNC interaction strength κ.

Since all allowed $|I-1| \leqslant F' \leqslant I+1$ final substates are degenerate in energy (within the approximations of Sec. IV), we may cast the total $2\,^1S_0 \to 2\,^3S_1$ cross section as the sum $\sigma_T = \sigma_{I+1} + \sigma_I + \sigma_{I-1}$ of all three possible hyperfine transitions, in the form

$$\sigma_T = 3(2I+1)\sigma(0)(1 + \lambda\mathcal{A}). \tag{33}$$

From this result it is evident that the total cross section σ_T depends linearly on the photon helicity λ. This occurrence suggests performing two separate sets of measurements of σ_T, which we name σ_+ and σ_-, employing, respectively, right ($\lambda = +1$) and left ($\lambda = -1$) polarized laser light. Extraction of the nsd PNC asymmetry $\mathcal{A}$ is in this way immediate, since

$$\begin{aligned}\mathcal{A} &\equiv \frac{\sigma_+ - \sigma_-}{\sigma_+ + \sigma_-} \\ &= \frac{(2I+3)\mathcal{K}_{I+1} + (2I+1)\mathcal{K}_I + (2I-1)\mathcal{K}_{I-1}}{3(2I+1)}. \end{aligned} \tag{34}$$

The coefficient $\mathcal{A}$ represents the ultimate physical observable in the proposed scheme and, as well as the coefficients $\mathcal{K}$, is proportional to the nsd PNC strength κ. Numerical results of the asymmetry $\mathcal{A}$ are presented in Table II for several isotopes of He-like ions in the interval $28 \leqslant Z \leqslant 35$. Since $\mathcal{A}$ depends on K, as defined in Eq. (4), whose sign is determined by the unknown value ℓ of the valence nucleon, the results for $\mathcal{A}$ are averaged over the two possible values of K. The maximum relative error introduced by the averaging procedure is 3.4%.

VI. EXPERIMENTAL REQUIREMENTS AND DISCUSSION

Up to now, we focused on the general theoretical background and motivations of a spin-dependent PNC study. In particular, we derived Eq. (34), which suggests that nsd effects can be induced through a stimulated $2\,^1S_0 \to 2\,^3S_1$ transition with circularly polarized laser light in He-like ions. We want now to draw the consequences of this outcome and discuss the requirements and implications for an actual experimental measurement.

First of all, let us mention that the asymmetry defined in Eq. (34) strongly depends on the nuclear spin I. As can be seen in Tables II and III, for a fixed Z, the asymmetry is larger for low-I nuclides. This correlation is particularly manifest in the Ge nuclides, where $\mathcal{A}$ decreases from 5.40×10^{-7} at $I = 1/2$ to 0.70×10^{-7} at $I = 9/2$, as well as in Se nuclides, with $\mathcal{A} = 4.66 \times 10^{-7}$ at $I = 1/2$, and $\mathcal{A} = 0.62 \times 10^{-7}$ at $I = 9/2$. We conclude that He-like ions with $I = 1/2$ are the best candidates for nsd PNC asymmetry experimental measurements in the laser-induced $2\,^1S_0 \to 2\,^3S_1$ transition.

TABLE II. Asymmetry factor $\mathcal{A} \equiv (\sigma_+ - \sigma_-)/(\sigma_+ + \sigma_-)$ for several isotopes with $28 \leqslant Z \leqslant 35$. The nuclide half-life ($t_{1/2}$), nuclear spin (I) and nuclear momentum (μ, expressed in nuclear magnetons) are taken from Ref. [33].

Ion	$t_{1/2}$	I	μ	$10^{-7}\mathcal{A}$
$^{57}_{28}$Ni	36 h	3/2	0.88	0.664 31
$^{61}_{28}$Ni	stable	3/2	−0.750 02	0.665 95
$^{65}_{28}$Ni	2.52 h	5/2	0.69	0.459 56
$^{60}_{29}$Cu	23.4 min	2	1.219 00	0.739 67
$^{61}_{29}$Cu	3.41 h	3/2	2.140 00	1.004 23
$^{62}_{29}$Cu	9.73 min	1	−0.380 00	1.288 34
$^{63}_{29}$Cu	stable	3/2	2.223 29	1.029 04
$^{64}_{29}$Cu	12.70 h	1	−0.217 00	1.326 57
$^{65}_{29}$Cu	stable	3/2	2.381 67	1.057 13
$^{66}_{29}$Cu	5.1 min	1	−0.282 00	1.348 74
$^{63}_{30}$Zn	18.1 min	3/2	−0.281 640	1.234 13
$^{65}_{30}$Zn	244.1 d	5/2	0.769 000	0.840 09
$^{67}_{30}$Zn	stable	5/2	0.875 479	0.859 60
$^{69}_{30}$Zn	13.86 h	9/2	1.140 000	0.51 262
$^{71}_{30}$Zn	3.9 h	9/2	1.040 000	0.521 30
$^{67}_{31}$Ga	78.3 h	3/2	1.850 700	1.832 83
$^{68}_{31}$Ga	68.1 min	1	0.011 750	2.294 55
$^{69}_{31}$Ga	stable	3/2	2.016 589	1.891 61
$^{71}_{31}$Ga	stable	3/2	2.562 266	2.011 31
$^{72}_{31}$Ga	14.1 h	3	−0.132 240	0.921 19
$^{69}_{32}$Ge	39.0 h	5/2	0.735 0000	1.208 88
$^{71}_{32}$Ge	11.2 d	1/2	0.547 0000	5.255 16
$^{73}_{32}$Ge	stable	9/2	−0.879 4677	0.700 81
$^{75}_{32}$Ge	82.8 min	1/2	0.510 0000	5.395 67
$^{69}_{33}$As	15 min	5/2	1.200 000	1.200 77
$^{70}_{33}$As	53 min	4	2.106 100	0.801 74
$^{71}_{33}$As	65.3 h	5/2	1.673 500	1.251 77
$^{72}_{33}$As	26 h	2	−2.156 600	1.278 89
$^{74}_{33}$As	17.78 d	2	−1.597 000	1.335 09
$^{75}_{33}$As	stable	3/2	1.439 475	2.086 91
$^{76}_{33}$As	26.3 h	2	−0.906 000	1.403 86
$^{73}_{34}$Se	7.1 h	9/2	0.8700 000	0.623 39
$^{75}_{34}$Se	118.5 d	5/2	0.6700 000	1.084 38
$^{77}_{34}$Se	stable	1/2	0.535 0422	4.663 09
$^{79}_{34}$Se	65000 yr	7/2	−1.018 0000	0.787 13
$^{74}_{35}$Br	41.5 min	4	1.450 000	1.086 62
$^{75}_{35}$Br	98 min	3/2	0.750 000	1.417 83
$^{76}_{35}$Br	16.1 h	1	0.548 210	2.018 82
$^{77}_{35}$Br	57.0 h	3/2	0.920 000	1.456 79
$^{79}_{35}$Br	stable	3/2	2.106 400	1.597 76
$^{80}_{35}$Br	17.6 min	1	0.514 000	2.080 26
$^{81}_{35}$Br	stable	3/2	2.270 562	1.642 04
$^{82}_{35}$Br	35.34 h	5	1.627 000	0.509 31
$^{83}_{36}$Kr	stable	9/2	−0.970669	0.44103
$^{85}_{36}$Kr	10.7 yr	9/2	1.000000	0.46161
$^{87}_{36}$Kr	76 min	5/2	−1.018000	0.76164

TABLE III. Einstein coefficients A and energies ΔE of the electromagnetic transitions among the first excited levels in He-like $^{77}_{34}$Se ions. The type "hf" given for $2\,^1S_0 \to 1\,^1S_0$ stands for hyperfine-induced transition.

Transition	Type	ΔE (eV)	A (s^{-1})	Ref.
$2\,^1S_0 \to 1\,^1S_0$	$2E1$	11579.4923	2.068×10^{10}	[34]
$2\,^1S_0 \to 2\,^3S_1$	$M1$	43.8529	1.16×10^{3}	[35]
$2\,^1S_0 \to 1\,^1S_0$	hf	11579.4923	587.21	[36]
$2\,^3S_1 \to 1\,^1S_0$	$2E1$	11535.6394	4.200×10^{9}	[37]
$2\,^3S_1 \to 1\,^1S_0$	$M1$	11535.6394	3.239×10^{9}	[38]
$2\,^3P_1 \to 1\,^1S_0$	$E1$	11579.2857	2.795×10^{14}	[38]
$2\,^3P_1 \to 2\,^3S_1$	$E1$	43.6463	5.614×10^{8}	[38]

Moreover, from the discussion in Sec. III, it is also clear that the splitting between the levels $2\,^1S_0$ and $2\,^3P_1$ should be as small as possible in order to maximize the mixing. It is also reasonable to require that the nuclides be stable, to avoid the complications of operating with radioactive beams. Based on these prerequisites, we argue that He-like $^{77}_{34}$Se ions are the most suitable candidates for the proposed scheme. The benefit of employing this isotope is that it is stable, it features a low nuclear spin ($I = 1/2$), and the energy splitting is just 206.58 meV (see Table I). The complete energy spectrum of the first excited levels in He-like $^{77}_{34}$Se has been already shown in Fig. 1, while we list in Table III numerical values of the dominant spontaneous decay rates.

Since we wish to study PNC $2\,^1S_0 \to 2\,^3S_1$ transitions, the aim is to make them strong enough to compete with spontaneous decay channels from the $2\,^1S_0$ state, by means of a laser of suitable intensity. For the $2\,^1S_0$ state, in particular, the PNC transition must compete with the $2E1$ decay to the ground state, whose rate is $2.068 \times 10^{10}\,s^{-1}$ (see Table III). Based on this condition, we can calculate the minimum required laser intensity.

Let us consider the rate $W_{2\,^1S_0 \to 2\,^3S_1}$ of the stimulated transition $2\,^1S_0 \to 2\,^3S_1$. This is proportional to the laser intensity I and obeys the relation [39]

$$W_{2\,^1S_0 \to 2\,^3S_1} = \frac{3}{4\pi^2} \frac{A_{2\,^1S_0 \to 2\,^3S_1}}{\Gamma_{2\,^1S_0}} \lambda^3_{2\,^1S_0 \to 2\,^3S_1} I. \tag{35}$$

In this formula, by employing the numerical data in Table III, $A_{2\,^1S_0 \to 2\,^3S_1} = 1.16 \times 10^3\,s^{-1}$ is the Einstein coefficient of spontaneous transition; $\Gamma_{2\,^1S_0} = \hbar A_{2\,^1S_0 \to 2\,^3S_1} + \hbar A_{2\,^1S_0 \to 1\,^1S_0} = 1.36 \times 10^{-5}$ eV the width of the initia state; and $\lambda_{2\,^1S_0 \to 2\,^3S_1} = 282.73$ Å the transition wavelength. Numerically, we obtain from Eq. (35) the law

$$W_{2\,^1S_0 \to 2\,^3S_1} = 0.03\,046\,986 I, \tag{36}$$

where the intensity I is measured in W/cm^2, and the transition rate $W_{2\,^1S_0 \to 2\,^3S_1}$ in s^{-1}.

The condition that the rate in Eq. (36) be faster than the decay to the ground state can be written as $W_{2\,^1S_0 \to 2\,^3S_1} > A_{2\,^1S_0 \to 1\,^1S_0} = 2.068 \times 10^{10}\,s^{-1}$. By inverting Eq. (36), this implies that the laser intensity I for a nsd PNC experiment in He-like $^{77}_{34}$Se should satisfy

$$I \geqslant I_{\min} = 6.79 \times 10^{11}\,W/cm^2. \tag{37}$$

The energy difference between levels $2\,^1S_0$ and $2\,^3S_1$ is 43.6463 eV in He-like $^{77}_{34}$Se, and therefore a laser in the EUV range is required to stimulate the transition. Pulsed sources of coherent EUV and soft x-ray light employing high harmonic generation with intensity in the range 10^{11}–10^{14} W/cm^2 are nowadays available [40], although polarization still remains an issue. Another possibility would be to employ vacuum ultraviolet (VUV) lasers, for which circular polarization is practicable (see, e.g., [41–43]), and exploit the Doppler effect such that the photon frequency in the ion's rest frame of reference matches the transition energy. All these laser sources offer a bandwidth of several eV, i.e., much wider than the sub-eV hyperfine structure of $2\,^3S_1$. This justifies our approximation of neglecting the hyperfine splitting on the $2\,^3S_1$ level.

For the feasibility of a measurement in our present scheme, it is essential to produce He-like ions in the $2\,^1S_0$ state. A technique for selective population in highly charged ions, based on inner-shell ionization and simultaneous single-electron excitation [44], was demonstrated for U ($Z = 92$) [45–48], and recently employed for elements as light as Sn ($Z = 50$) [49,50] and Au ($Z = 79$) [51]. Alternatively, another way also employs dielectronic recombination of H-like ions into $(2s2p)\,^1P_1$, since the latter state decays promptly into $2\,^1S_0$. This method has been already successfully adopted with He-like Ge [52], i.e., in the Z range considered in this work.

As far as detection of the induced $2\,^1S_0 \to 2\,^3S_1$ transition is concerned, we may notice that $2\,^3S_1$ decays to the ground state either by emission of a single $M1$ photon or two $2E1$ photons (see Fig. 1), with rates 3.239×10^9 and 4.200×10^9 s^{-1}, respectively (cf. Table III). Detection of the $2E1$ decay, although viable [50], is unpractical since its energy spectrum may be contaminated by two-photon decay from $2\,^1S_0$ to the ground state. Instead, detection of a single photon of fixed energy 11.536 keV in the $M1$ decay would provide an ideal experimental signature of the $2\,^1S_0 \to 2\,^3S_1$ transition. The background is in this case rather suppressed, because $2\,^3S_1$ is well isolated from other levels and therefore no additional photon of comparable energy is expected. As a drawback, however, only $A_{M1}/A_{2E1} = 43.5\%$ of the $2\,^1S_0 \to 2\,^3S_1$ events can be tagged, and a high statistics is required for precise measurement of nsd PNC asymmetry.

VII. CONCLUSIONS

In this paper we analyzed a scheme for the investigation of nuclear-spin-dependent parity-nonconservation in He-like ions. We showed that an interference between $M1$ and $E1$ multipoles in the laser-stimulated $2\,^1S_0 \to 2\,^3S_1$ transition leads to an observable parity-violating asymmetry in the cross section, when alternately left and right circularly polarized light is employed. This effect is especially amplified in $28 \leqslant Z \leqslant 36$ ions of nuclear spin $I = 1/2$. The maximum value of parity-violation asymmetry is found in the two unstable $A = 71$ and $A = 75$ isotopes of germanium, as well as in the $A = 77$ isotope of selenium. The latter is stable and may be conveniently employed in a future experiment at storage rings.

The $2\,^1S_0 - 2\,^3S_1$ transition energy in $^{77}_{34}$Se is 43.6463 eV, which requires EUV lasers with an intensity of order 10^{11} W/cm^2. Although adequate laser sources are available, the circular polarization of their light still poses technical problems.

As a tagging of the transition, we suggest using the spontaneous decay of the $2\,^3S_1$ level to the ground state. This occurs through emission of either two photons or a single $M1$ photon with approximately equal probability. Detection of the $M1$ decay photon of ~ 11.5 keV energy represents the simplest and most convenient signature of the laser-induced transition, thanks to low background. This can be performed employing today's high-accuracy spectroscopy methods at storage rings.

ACKNOWLEDGMENTS

The authors gratefully thank Dr. Luca Argenti for constructive and enlightening discussions. F.F. and A.S. acknowledge support by the Helmholtz Association and GSI under the project VH-NG-421, and T.S. by the ExtreMe Matter Institute EMMI in the framework of the Helmholtz Alliance HA216/EMMI.

[1] W. J. Marciano and J. L. Rosner, Phys. Rev. Lett. **65**, 2963 (1990); **68**, 898 (1992).
[2] M. J. Ramsey-Musolf, Phys. Rev. C **60**, 015501 (1999).
[3] S. G. Porsev, K. Beloy, and A. Derevianko, Phys. Rev. Lett. **102**, 181601 (2009).
[4] I. B. Khriplovich, *Parity Nonconservation in Atomic Phenomena* (Gordon and Breach Science, Philadelphia, 1991).
[5] J. S. M. Ginges and V. V. Flambaum, Phys. Rep. **397**, 63 (2004).
[6] Ya. B. Zeldovich, Sov. Phys. JETP **6**, 1184 (1958).
[7] V. V. Flambaum and I. B. Khriplovich, Sov. Phys. JETP **52**, 835 (1980).
[8] V. V. Flambaum, I. B. Khriplovich, and O. P. Sushkov, Phys. Lett. B **146**, 367 (1984).
[9] C. Bouchiat and C. A. Piketty, Phys. Lett. B **269**, 195 (1991).
[10] W. R. Johnson, M. S. Safronova, and U. I. Safronova, Phys. Rev. A **67**, 062106 (2003).
[11] C. S. Wood, S. C. Bennett, D. Cho, B. P. Masterson, J. L. Roberts, C. E. Tanner, and C. E. Wieman, Science **275**, 1759 (1997).
[12] P. A. Vetter, D. M. Meekhof, P. K. Majumder, S. K. Lamoreaux, and E. N. Fortson, Phys. Rev. Lett. **74**, 2658 (1995).
[13] D. Sheng, L. A. Orozco, and E. Gomez, J. Phys. B **43**, 074004 (2010).
[14] E. N. Fortson, Y. Pang, and L. Wilets, Phys. Rev. Lett. **65**, 2857 (1990).
[15] M. Maul, A. Schäfer, W. Greiner, and P. Indelicato, Phys. Rev. A **53**, 3915 (1996).
[16] R. W. Dunford, Phys. Rev. A **54**, 3820 (1996).
[17] V. G. Gorshkov and L. I. Labzovski, Zh. Eksp. Teor. Fiz., Pis'ma Red. **19**, 768 (1974)[JETP Lett. **19**, 394 (1974)].
[18] F. Ferro, A. Artemyev, T. Stöhlker, and A. Surzhykov, Phys. Rev. A **81**, 052112 (2010).
[19] F. Ferro, A. Artemyev, T. Stöhlker, and A. Surzhykov, J. Instrum. **5**, C08006 (2010).

[20] A. V. Nefiodov, L. N. Labzowsky, D. Liesen, G. Plunien, and G. Soff, Phys. Lett. B **534**, 52 (2002).
[21] V. M. Shabaev, A. V. Volotka, C. Kozhuharov, G. Plunien, and Th. Stöhlker, Phys. Rev. A **81**, 052102 (2010).
[22] M. G. Kozlov, Phys. Lett. A **130**, 426 (1988).
[23] V. V. Flambaum and C. Hanhart, Phys. Rev. C **48**, 1329 (1993).
[24] V. V. Flambaum and D. W. Murray, Phys. Rev. C **56**, 1641 (1997).
[25] S. C. Bennett and C. E. Wieman, Phys. Rev. Lett. **82**, 2484 (1999).
[26] W. C. Haxton, C.-P. Liu, and M. J. Ramsey-Musolf, Phys. Rev. Lett. **86**, 5247 (2001); Phys. Rev. C **65**, 045502 (2002).
[27] G. Feinberg and M. Y. Chen, Phys. Rev. D **10**, 190 (1974).
[28] I. Lindgren and J. Morrison, *Atomic Many-Body Theory* (Springer-Verlag, Berlin, 1982).
[29] K. T. Cheng and W. J. Childs, Phys. Rev. A **31**, 2775 (1985).
[30] F. Ferro, A. Artemyev, A. Surzhykov, and T. Stöhlker, Can. J. Phys. **89**, 73 (2011).
[31] A. N. Artemyev, V. M. Shabaev, V. A. Yerokhin, G. Plunien, and G. Soff, Phys. Rev. A **71**, 062104 (2005).
[32] J. D. Jackson, *Classical Electrodynamics*, 3rd ed. (Wiley, New York, 1998).
[33] N. J. Stone, At. Data Nucl. Data Tables **90**, 75 (2005).
[34] A. Derevianko and W. R. Johnson, Phys. Rev. A **56**, 1288 (1997).
[35] C. D. Lin, W. R. Johnson, and A. Dalgarno, Phys. Rev. A **15**, 154 (1977).
[36] J. G. Li, P. Jönsson, G. Gaigalas, and C. Z. Dong, Eur. Phys. J. D **51**, 313 (2009).
[37] H. W. Schäffer, R. W. Dunford, E. P. Kanter, S. Cheng, L. J. Curtis, A. E. Livingston, and P. H. Mokler, Phys. Rev. A **59**, 245 (1999).
[38] W. R. Johnson, D. R. Plante, and J. Sapirstein, Adv. At. Mol. Opt. Phys. **35**, 255 (1995).
[39] A. E. Siegman, *Lasers* (University Science Books, Mill Valley, CA, 1986).
[40] E. A. Gibson *et al.*, Science **302**, 95 (2003).
[41] H. Rottke and H. Zacharias, Phys. Rev. A **33**, 736 (1986).
[42] R. Irrgang, M. Drescher, F. Gierschner, M. Spieweck, and U. Heinzmann, Meas. Sci. Technol. **9**, 422 (1998).
[43] L. Muser, C. Olivero, D. Riedel, and M. C. Castex, Appl. Phys. B **70**, 499 (2000).
[44] A. Surzhykov, U. D. Jentschura, T. Stohlker, A. Gumberidze and S. Fritzsche, Phys. Rev. A **77**, 042722 (2008).
[45] D. Banas *et al.*, Nucl. Instrum. Methods B **235**, 326 (2005).
[46] J. Rzadkiewicz *et al.*, Phys. Rev. A **74**, 012511 (2006).
[47] S. Trotsenko *et al.*, J. Phys. Conf. Ser. **58**, 141 (2007).
[48] J.-J. Wan, C.-Z. Dong, X.-B. Ding, X.-W. Ma, J. Rzadkiewicz, T. Stöhlker and S. Fritzsche, Phys. Rev. A **79**, 022707 (2009).
[49] A. Kumar *et al.*, J. Phys. Conf. Ser. **163**, 012027 (2009).
[50] S. Trotsenko *et al.*, Phys. Rev. Lett. **104**, 033001 (2010).
[51] A. Gumberidze, S. Fritzsche, F. Bosch, D. C. Ionescu, A. Kramer, C. Kozhuharov, Z. Stachura, Z. Stachura, A. Warczak and T. Stohlker, Phys. Rev. A **82**, 052712 (2010).
[52] P. H. Mokler, S. Reusch, A. Warczak, Z. Stachura, T. Kambara, A. Müller, R. Schuch, and M. Schulz, Phys. Rev. Lett. **65**, 3108 (1990).